Potential Energy Savings of Various Roof Technologies

Stephen Ray
Student Member ASHRAE

Leon Glicksman, PhD
Fellow ASHRAE

ABSTRACT

Previous studies suggest potential for energy savings through cool and green roofs but do not always consider the many factors that affect potential savings or the relative advantages of different technologies. To further investigate these factors, a tool has been developed to allow architects the ability to quickly assess the energy-saving potential of different roof systems. A first-principles heat transfer model has been developed for each of the roof technologies, with particular care for green roof heat and mass transfer. Experimental data from Japan and Florida validate the models by predicting roof surface temperatures.

Example simulations are run with the tool to show that potential energy savings are highly sensitive to many parameters, particularly roof type, climate, and amount of insulation. To illustrate these dependencies, simulations show that a one-story building in Boston with a modified-bitumen roof and 2.7 m^2K/W roof insulation can save 13% in cooling and heating energy by doubling the insulation, whereas only 12% can be saved if a green roof is installed instead. However, in Lisbon, the same additional amount of roof insulation to the same building results in –0.010% savings, while the installation of a green roof results in a 26% reduction in energy use.

INTRODUCTION

Alternative roof solutions, such as green and cool roofs, are rapidly finding their way atop more buildings each year. One reason for this growth is their potential energy savings.

Previous Work

Extensive experimental work has been completed to show the potential energy savings of these types of roofs, but little comparative work between technologies or evaluation of the impact of roof insulation has been done. In addition to experimental work, numerous models have been developed to simulate the energy performance of these alternative roofs. However, many models remain unhelpful to building decision makers due to their complexity, required software familiarization, or simple lack of public availability (Zhang et al. 1997; Niachou et al. 2001; Lazzarin et al. 2005; Santamouris et al. 2007; Takakura 1993; Alexandri and Jones 2007; Takakura 2000; Theodosiou 2003; Kumar and Kaushik 2005; Wong et al. 2003). Sailor's (2008) work on green roofs comes close to being accessible to decision makers, as it incorporates a comprehensive green roof model into the EnergyPlus simulation engine (LBNL 2010). Additionally, Oak Ridge National Laboratory's AtticSim (Petrie and Wilkes 1998), which has been incorporated into DOE-2.1E (JJH 2003), predicts energy savings of cool roofs (LaFrance et al. 2010). Unfortunately, the required level of expertise for EnergyPlus and DOE-2.1E is a significant hurdle for nontechnical users, including many building decision makers. Building decision makers can rely on other sources to predict the energy savings associated with green or cool roofs. Green Roofs for Healthy Cities (GRHC), the Athena Institute, and Tremco Roofing and Building Maintenance have developed a free online tool that compares "roofing alternatives over a specific time period to determine which has the lowest life-cycle cost" (GHRC 2009). However, it grossly oversimplifies the energy savings by forcing users to

Stephen Ray *is a PhD student in the Department of Mechanical Engineering and* ***Leon Glicksman*** *is a professor of Building Technology and Mechanical Engineering at Massachusetts Institute of Technology, Cambridge, MA.*

choose one of three reported energy consumption values from green-roofed buildings in three climates.

Decision makers can also rely on guidebooks for a "rule of thumb," but such generalities often neglect other building aspects, such as the envelope and internal gains. In order to equip building decision makers with a tool simple enough for nontechnical users but detailed enough to provide accurate information relevant to their buildings, a new roof module has been added to MIT's existing free online building simulator, Design Advisor (MIT 2010). This roof module has been developed to allow comparison between different roof technologies—comparison that is often not made in work that focuses on how one specific technology compares to a conventional roof. Other oft-neglected considerations addressed by this work are building components such as roof insulation amount and location, along with the number of floors in a building, which all affect the total building energy use.

The MIT Design Advisor

The single-page interface of the MIT Design Advisor (MIT 2010) allows technical and nontechnical users alike to quickly and accurately model building energy use and has been previously shown to be accessible to building decision makers (Urban 2007). More information on the MIT Design Advisor is available online at http://designadvisor.mit.edu and in Urban's (2007) thesis.

Outline

The work presented in this paper uses a first-principles-based model to estimate the energy flux through the roof that is used in the HVAC loads module of the MIT Design Advisor. Two roof models are developed, one for modified-bitumen and cool roofs, where a cool roof is defined as in ASHRAE/IESNA Standard 90.1 as having a minimum solar reflectance of 0.70 and minimum thermal emittance of 0.75 (hereafter referred to as the *cool roof model*) (ASHRAE 2004). The second model (*green roof model*) is for extensive green roofs, defined as a vegetated roof with 1–6 inches of soil. The models are derived and validated before implications of this work are discussed.

ROOF ENERGY MODEL

Cool and Modified-Bitumen Roof Model

The similar construction of both cool and modified-bitumen roofs allows for a single cool roof model to be used for both roofs, in which only roof surface reflectivity (ρ) is altered. The cool roof model assumes one-dimensional heat transfer through the roof, which is assumed to have an area large enough that edge effects are neglected, as are the thermal resistances of any surface coating or waterproofing layers. The roof model is composed of a 15 cm thick concrete slab with a variable amount of insulation on top of or beneath the slab. In both cases, as shown in Figure 1, the upper surface of the roof, which is assumed to be a gray body, is exposed to incident shortwave radiation from the sun (I_s), longwave radiation exchange with the sky ($q_{ir,roof}$), and convective heat exchange with the outside environment (H_{roof}), all of which are in watts per square meter. When insulation is placed above the roof structural slab, a 1/2 in. cover board protects the insulation from the environment and thus is the topmost layer, with a conductivity of 0.133 W/m·K, density of 746 kg/m^3, and heat capacity of 1090 J/kg·K.

The sky is assumed to be a black body at a temperature of 10 K below the ambient temperature (Martin and Berdahl 1984). This assumption allows the linearization of the longwave radiation heat transfer between the roof surface and the assumed sky temperature that results in the following (Lienhard and Lienhard 2006):

$$q_{ir,\,roof} = 4\varepsilon\sigma T_m^3 (T_{sky} - T_{surface}) \quad (1)$$

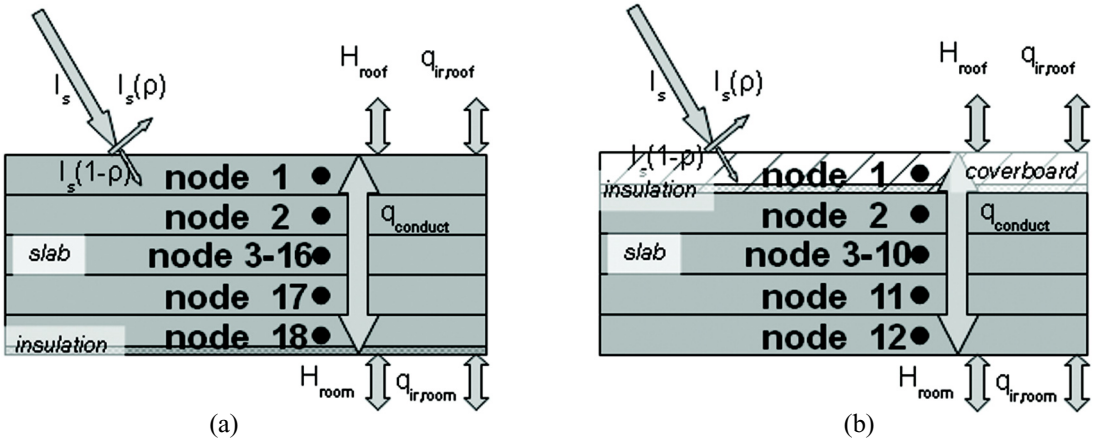

Figure 1 *Nodal schematic for the cool roof model when roof insulation is a) below and b) above the roof structural slab, corresponding to the bottoms of nodes 18 and 1, respectively. Note the cover board used in the latter case.*

where ε is the emissivity of the roof, σ is the Stefan-Boltzman coefficient, and T_m is the average temperature of the roof surface and the sky. Although T_m changes slightly throughout the day and depending on location, any change is relatively small compared to the absolute temperature; thus, T_m is assumed to be a constant 303 K to enable faster calculations. The convection term H_{roof} is assumed to be purely forced convection and is found using an average heat transfer coefficient as follows:

$$H_{roof} = \bar{h}(T_{amb} - T_{surface}) \tag{2}$$

where T_{amb} is the ambient outdoor temperature in K. After calculating $\bar{h}$ from the average Nusselt number for turbulent flow over a flat plate for numerous wind speeds typical on roofs, it is found that the variation in $\bar{h}$ has a negligible effect on the total heat transfer to the roof. Thus, $\bar{h}$ is assumed to equal a constant 10 W/m^2·K, corresponding to an average wind speed on the roof just under 5 m/s and a roof length of 25 m (Mills 1991). The thermally massive concrete is assumed to have constant conductivity along with the insulation. In contrast, the insulation has a thermal mass that is negligible compared to the mass of the concrete, so it is omitted; accounting for it would noticeably increase the complexity of the model (Smith 2004). Longwave radiation and convective heat transfer are the two modes of thermal interaction between the topmost room of the building, assumed to be of uniform temperature T_{room}, and the ceiling, the underside of the roof. The small temperature difference between the room and ceiling justifies the linearization of the radiative heat transfer, which is combined with the convection term to form an effective heat transfer coefficient from the ceiling to the room, h_{room}. Based on Urban's (2007) justifications, h_{room} is approximated as a constant 10 W/m^2·K.

Cool and Modified-Bitumen Roof Nodal Energy Balance

To account for the transient temperature gradient in the concrete while minimizing calculation complexity, the concrete is divided into numerous thin slices, each modeled with a lumped capacitance to which an energy balance is applied. Slice thickness is chosen to ensure the Biot Number is less than 0.1 for the outer slices to satisfy the lumped capacitance criterion. The determined slice thickness is used to calculate the appropriate time step for the energy balance such that the Fourier Number is less than 0.5, justifying the constant temperature assumption over the time step. Each node interacts with neighboring nodes purely through conduction. The nodal schematics for the cool roof model with roof insulation above and below the roof structural slab are shown in Figure 1.

The energy balance for each node is discretized using the Crank-Nicolson method, which averages the current and predicted next time step's nodal temperature (Urban 2007; Strang 2007).

Combining the discretized equations for all nodes, a system of equations is created where nodal temperatures can be predicted as a function of time and position using input weather parameters and an initial temperature distribution in the slab. Once the temperature of the final node is known, the heat flux to the room beneath is simply calculated given h_{room} and a known T_{room}.

Green Roof Energy Model

In the green roof model, the same assumption for one-dimensional heat transfer that neglects edge effects is used as before, but this time the vegetation and growing media must be considered.

The vegetation is assumed to be a cool-season, clipped grass covering the entire roof with evapotranspiration modeled by the reference case of the FAO-56 Penman-Monteith equation (PM), defined as (Allen et al. 1998):

$$ET_0 = \frac{0.408\Delta(R_n - G) + \gamma\frac{37}{T_{hr}}u_2(P_{sat(T_{hr})} - P_{act})}{\Delta + \gamma(1 + 0.34u_2)} \tag{3}$$

where

ET_0 = the reference evapotranspiration, mm/h
R_n = the net radiation at the grass surface, MJ/m^2·h
G = the soil conductive heat flux density, MJ/m^2·h
T_{hr} = the mean hourly air temperature, °C
Δ = the saturation slope vapor pressure curve at T_{hr}, kPa/°C
γ = the psychrometric constant, kPa/°C
$P_{sat(T_{hr})}$ = the saturation vapor pressure at T_{hr}, kPa
P_{act} = the average hourly actual vapor pressure, kPa
u_2 = the average hourly wind speed 2 m above the vegetation, m/s

The PM assumes vegetation is always actively living, a requirement of which is weekly irrigation, and uses weather input parameters to predict the amount of water evapotranspired by cool-season clipped grass (Allen et al. 1998). The PM is often used as the standard to which other evapotranspiration models are compared, which justifies its use here (Droogers and Allen 2002; Kite and Droogers 2000; Suleiman and Hoogenboom 2007).

In the current model, radiation through the vegetation is described by the Beer-Lambert law, which defines the vegetation transmittance τ as

$$\tau \equiv \exp(-\sqrt{\alpha} \cdot k_{ext} \cdot \mathrm{LAI}) \quad , \tag{4}$$

where α is the fraction of light absorbed by an individual leaf, k_{ext} is the vegetation extinction coefficient, and LAI is the leaf area index of the vegetation (Teh 2006; Russell et al. 1990). Both α and k_{ext} can vary with wavelength; thus, two values for each are used, a_s and a_l and $k_{ext,s}$ and $k_{ext,l}$, for shortwave and longwave radiation, respectively. Additionally, both values

are most often empirically measured, as they are in this model. The leaf area index, LAI, is the total leaf area per unit ground area (Teh 2006) and is defined in this case using

$$\mathrm{LAI} = 24 \cdot height_{grass} \ , \tag{5}$$

where $height_{grass}$ is the grass height in m (Allen 2005). Using this definition of τ and the collective reflectance of the vegetated surface ρ_{veg}, which is taken from the PM, the incident solar radiation to the vegetation $I_{s,veg}$ is defined as

$$I_{s,\,veg} = (1-\rho_{veg})I_s(1-\tau_s) \ . \tag{6}$$

Assuming all incident solar radiation not reflected back to the sky is either absorbed by the vegetation or passes through to the soil, the incident solar radiation to the soil is

$$I_{s,\,soil} = \alpha_{soil}(1-\rho_{veg})I_s \cdot \tau_s \ , \tag{7}$$

where α_{soil} is the absorptivity of the soil, which is assumed to have relatively constant thermal properties over time given the assumption of actively living grass. The longwave radiation heat transfer between the vegetation and sky is

$$q_{ir,\,veg} = (1-\tau_l) \cdot h_{rad}(T_{veg} - T_{sky}) \tag{8}$$

and between soil and sky is

$$q_{ir,\,veg} = \tau_l \cdot h_{rad}(T_{veg} - T_{sky}) \ . \tag{9}$$

Any interaction between the vegetation and soil is assumed to be through longwave radiation $q_{ir,soil\text{-}veg}$:

$$q_{ir,\,soil-veg} = (1-\tau_l) \cdot h_{rad}(T_{veg} - T_{soil}) \tag{10}$$

The vegetation is assumed to have a heat capacity per leaf square meter of 640 J/m^2·K, which Jones (1992) found for the general plant leaf.

Green Roof Nodal Energy Balance

The same lumped capacity nodal analysis from before is also used in the green roof model, with the nodes shown in Figure 2, where all terms have been previously defined except H_{veg} and L_{veg}. The convective heat transfer from the vegetation to the environment, H_{veg}, is similarly defined as H_{roof} in the cool roof model, except it accounts for leaf surface area:

$$H_{veg} = \bar{h}\frac{\mathrm{LAI}}{2}(T_{amb} - T_{veg}) \tag{11}$$

The latent heat transfer from the vegetation, L_{veg}, is found by first assuming all of the estimated evapotranspiration occurs as transpiration because the vegetation is assumed to cover the entire roof and be actively living. L_{veg} is then easily found by converting ET_0 to an energy flux in watts per square meter using the latent heat of vaporization of water.

As indicated by the single node for vegetation in Figure 2, all of the vegetation is taken to be at a single temperature T_{veg} that is distinct from the soil surface temperature. The vertical temperature gradient through the soil is considered by dividing it into nodal slices as is done for the concrete. Figure 2 also shows that the only interaction between the vegetation and soil surface (nodes 1 and 2) is through long-

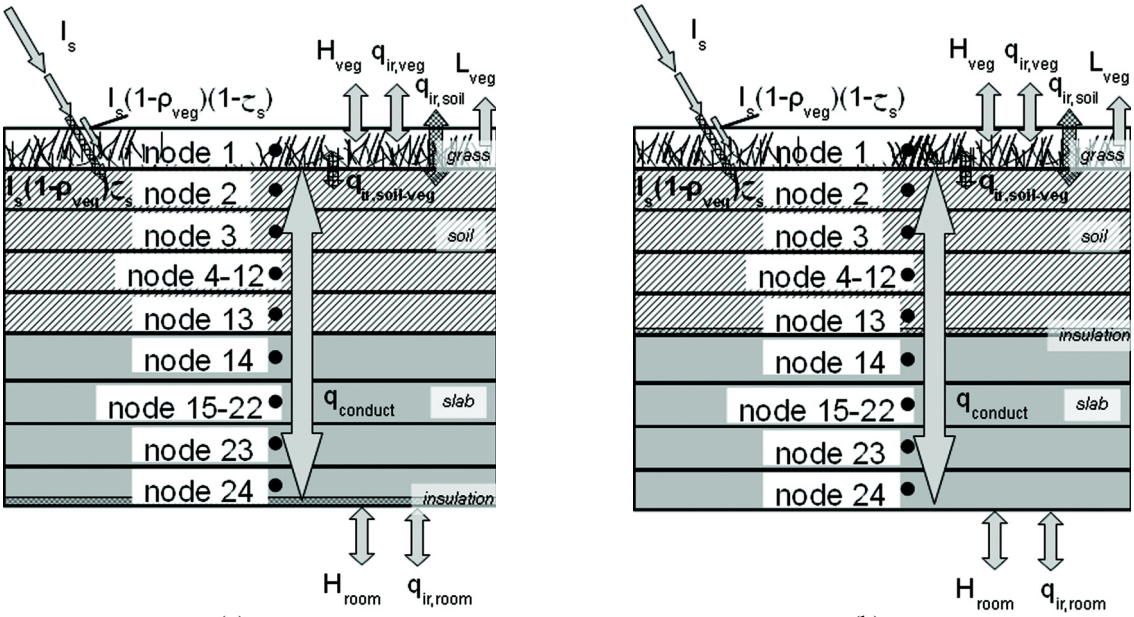

Figure 2 *Nodal schematic for the green roof model when roof insulation is a) below and b) above the roof structural slab, corresponding to the bottom of node 24 and between nodes 13–14, respectively.*

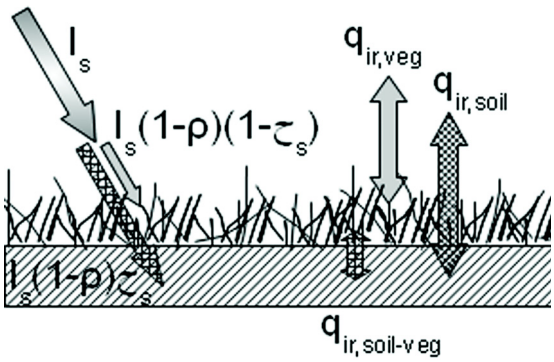

Figure 3 *Enlarged view of interaction between vegetation and soil layers.*

wave radiation ($q_{ir,soil-veg}$), though every subsequent node interacts solely through conduction. An enlarged view of the vegetation and soil layers is shown in Figure 3.

Similar to the cool roof model, an energy balance is applied to each node and then discretized before being combined with all nodes to create a system of equations defined by Equation 6. As before, the roof temperature can be predicted using input weather parameters and an initial temperature distribution throughout the nodes.

MODEL VALIDATION

To prove both the generality and the specificity of the models, two sets of experimental data that were obtained from different regions of the world, graciously shared by Jeff Sonne of the Florida Solar Energy Center (FSEC) and Professor Hideki Takebayashi of Kobe University, are used for validation. Although the models ultimately predict the energy flux into the building associated with either type of roof, which is unmeasured, the roof surface temperature is used to validate the models because of the linear relationship between the two values.

Experimental Setup

FSEC Experiment. One half of the 3300 ft^2 FSEC roof was a conventional, light-colored built-up roof with reflectivity of 0.50. The other half of the built-up roof was covered with native Floridian vegetation up to 0.61 m in height (Cummings et al. 2007; Sonne 2006; FSEC 2008). Although the green roof model assumes a 12 cm clipped grass, this difference in vegetation tests the generality of model.

Temperature measurements were taken at the roof surface, the bottom of the roof deck, the ambient air, the interior air, and the green roof growing media surface, with an accuracy of ±1.4°C. Roof insulation is used under the entire roof deck, though it equals 2.97 $W/m^2 \cdot K$ at the sensor locations used for this validation. Meteorological measurements taken on site include ambient air temperature, rainfall, total horizontal solar radiation, and wind speed and direction. The green roof was irrigated between 0.5 and 1.5 in. per week, so the soil was not lacking water as is assumed in the green roof model (Sonne 2008). Although the FSEC study did not measure humidity, hourly outdoor relative humidity data collected from the Orlando weather station were obtained from Weather Underground and the National Severe Storms Laboratory (WU 2008; Zhu and Schultz 2009). Data collected during both summer (July 17–23 and August 4–11, 2006) and winter (February 3–9, 2006) are used to test the validity of the models in both seasonal extremes.

University of Kobe Experiment. Hideki Takebayashi and Masakazu Moriyama of Kobe University investigated numerous kinds of roof technologies on the roof of a university building on their campus from July 2003 through February 2006 (Takebayashi and Moriyama 2007). The total uninsulated roof area of 42.9 m^2 was covered with numerous roof technologies, though only the extensive turf grass green roof, a bare concrete roof, and a white cool roof (with the measured reflectivity of the concrete and white cool roofs equaling 0.37 and 0.74, respectively) are considered in validating the models at hand (Takebayashi and Moriyama 2007). The short turf grass tests the generality of the green roof model.

Measurements taken included growing media surface, roof surface, and sofit temperatures. They also included weather parameters gathered at a nearby weather facility: ambient air temperature, relative humidity, and incident radiation (Takebayashi and Moriyama 2007). Data used from the Kobe University experiment were taken over three days, from August 27–29, 2004.

Validation

Measured local weather data and roof constructions are inputs to the model, which predicts $T_{surface}$, which is compared to the experimentally measured value. Furthermore, although the vegetation in the studies differs (recall that native plants of 0.61 m height are used in Florida and a short turf is used in Japan), the vegetation and its evapotranspiration in the green roof model are not changed in any way to better simulate either case. Rather, they are held constant to show that the green roof model can simulate various kinds of green roof vegetation with relative accuracy.

A substantial correlation between the cool roof model and the experimental data is shown in Figures 4 through 6, including error analysis, where required information is available, in Florida (Ray 2010). When predicting $T_{surface}$ for the FSEC and University of Kobe studies, the predicted roof surface temperature of the model agrees with the measured value within 7.2% and 10%, respectively, of the diurnal $T_{surface}$ fluctuation.

Like the cool roof model predictions, the green roof model predictions closely follow the experimental $T_{surface}$ (soil temperature in Florida and the vegetation temperature in Japan), as shown in Figures 4 through 6. The green roof model predicts surface temperatures that agree with measured values within 14% and 26% of diurnal $T_{surface}$ fluctuations in Florida and Japan, respectively. Although the Japanese experiment has vegetation more similar to that of the model, the lack of

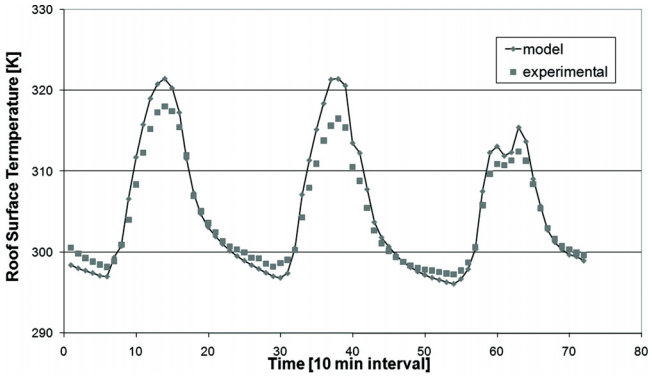

(a)

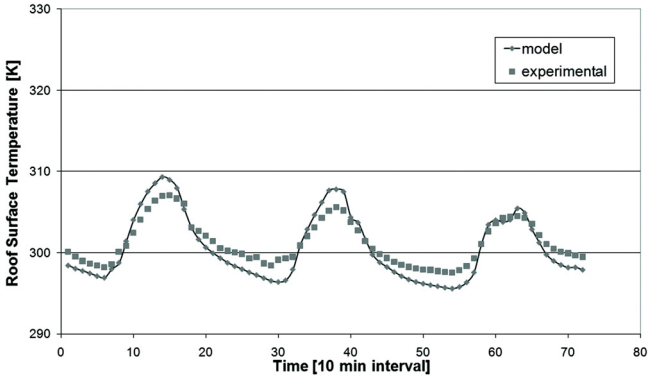

(b)

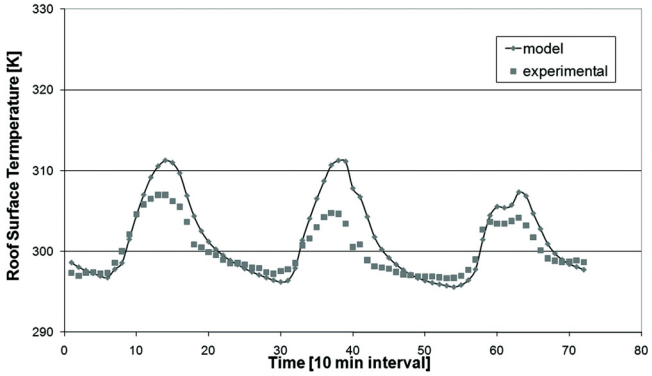

(c)

Figure 4 *Simulated and experimental* $T_{surface}$ *for a) a concrete roof, b) a cool roof, and c) an extensive turf roof in Japan during August 27–29, 2004 (Takebayashi and Moriyama 2006).*

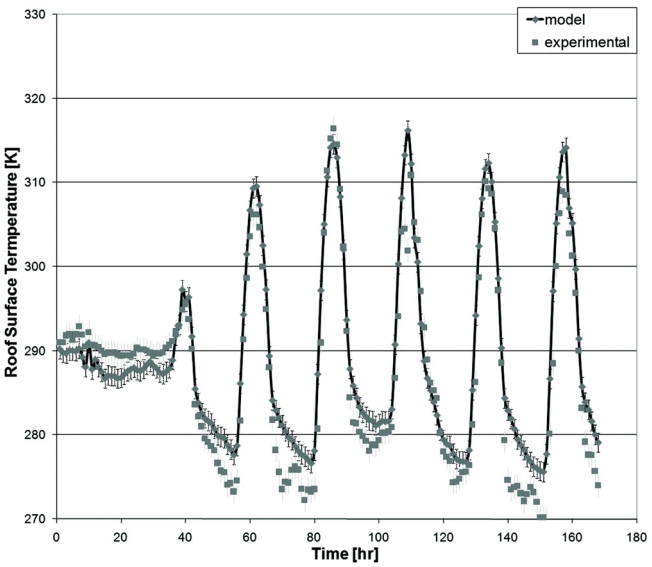

(a)

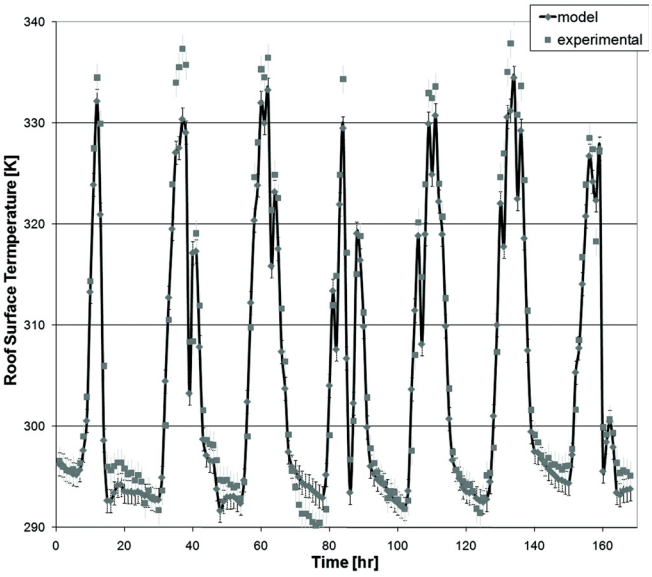

(b)

Figure 5 *Simulated and experimental* $T_{surface}$ *for the cool roof in Orlando, Florida, from a) February 3–9, 2006, and b) July 17–23, 2006. Experimental temperatures are accurate to ±1.4°C, while simulated temperatures are accurate to ±1.16°C, or 7.2% of the diurnal fluctuation (FSEC 2008).*

roof insulation there increases the sensitivity of the model to material properties, for which general values are used in the model. This increased sensitivity to unmeasured properties, particularly concrete thermal properties, is the likely cause of the poorer performance of both cool and green models in Japan. By varying the concrete thermal properties over the normal range for concrete, the experimentally measured temperatures are actually bounded.

This correlation validates not only the model's ability to predict green roof surface temperatures but also the model's generality by modeling two green roofs of different vegetation sufficiently well. As with the cool roof model, the ability to predict $T_{surface}$ leads to the prediction of the heat flux into the building.

RESULTS

Both roof models are incorporated into the existing building simulation tool, the MIT Design Advisor (MIT 2010), which is used to generate the following results.

Roof Types in Different Climates

Two parameters that greatly affect the energy savings attributable to roofs are the roof type and the local climate.

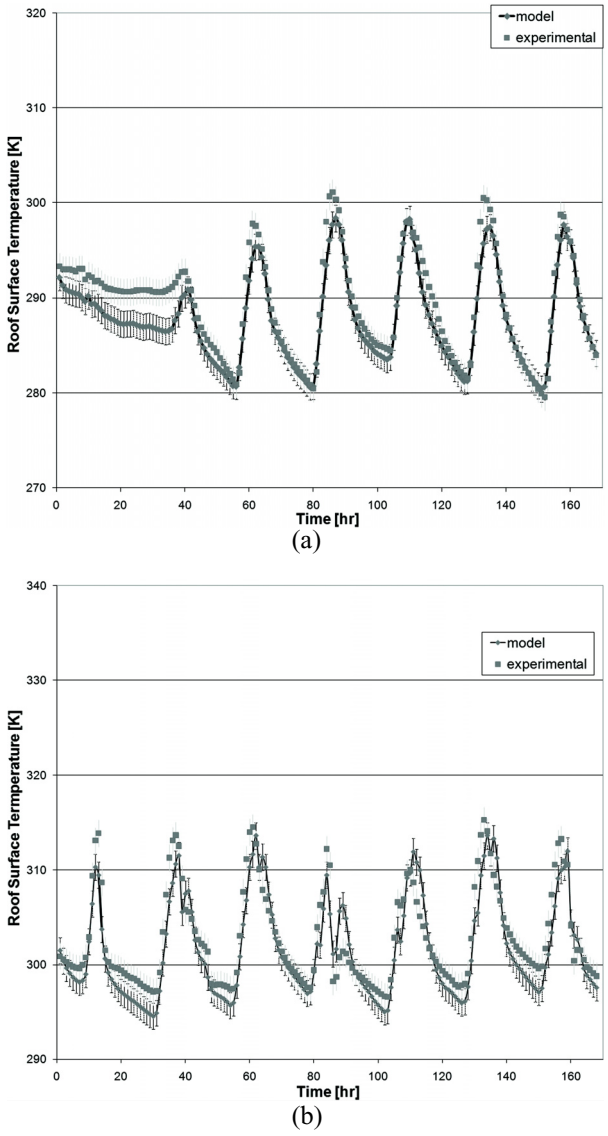

Figure 6 *Simulated and experimental soil surface temperatures for an extensive green roof in Orlando, Florida, during a) February 3–9, 2006, and b) July 17–23, 2006. Experimental temperatures are accurate to ±1.4°C while simulated temperatures are accurate to ±1.38°C, or 14% of the diurnal* $T_{surface}$ *fluctuation (FSEC 2008).*

Figure 7 shows the annual heating and cooling energy consumption for a simulated single-story, long, south-facing building with no roof insulation in various representative climates with a flat green roof, a cool roof, and a modified-bitumen roof. The building is 40% glazed only on the south facade, has low-e double-pane windows, has 2 $m^2 \cdot K/W$ exterior wall insulation, is ventilated at 0.5 ach, and has minimal internal loads of 7 W/m^2.

In the cold climates of Minneapolis and Boston, the cool roof performs roughly the same as the modified-bitumen roof. This equality in energy demand results from an increased heating load for the building with a cool roof because less of the sun's heat enters the building. Not just isolated to buildings in cold climates, this increase in heating energy occurs in every city when a cool roof is used. In a hot climate such as Phoenix, the cool roof nearly halves the energy consumption of the building with a traditional roof by reducing cooling needs. In cities with moderate climates, such as St. Louis and Lisbon, switching to a cool roof leads to at least minimal savings. In each of the five cities considered, the green roof leads to the lowest energy consumption, as the soil helps insulate the roof that otherwise has no insulation.

In addition to the insulative effect of the soil, because the vegetation is assumed to always be healthy, the green roof provides passive cooling to the roof when the incident radiation and ambient temperature are high enough to allow evapotranspiration. The water required for this evapotranspiration varies significantly with location, climate, and time of year. However, in the most extreme conditions considered, during the Phoenix summer, a weekly irrigation rate of 3.3 in. is needed to allow the modeled evapotranspiration. This weekly rate averages to 13 in./month of required water in the summer, of which 0.99 in. could be met by the average July precipitation at the Phoenix Sky Harbor International Airport (NWS 2009). The large effect

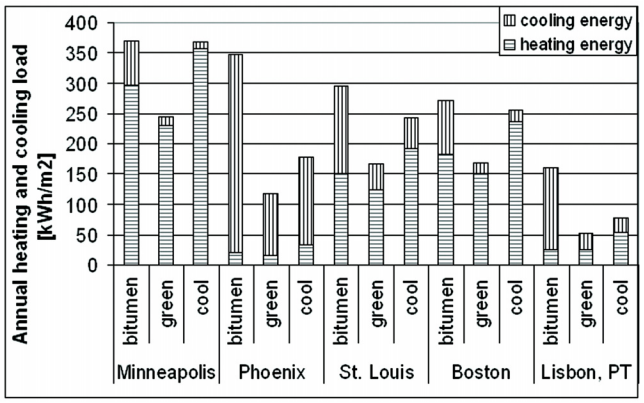

Figure 7 *Average annual primary energy required for heating and cooling a single-story building with a flat roof, no roof insulation, 40% glazing, light thermal mass, and mechanical heating and cooling systems.*

of roof type on energy consumption, up to a 60% reduction, suggests enormous energy savings potential by changing roofs, particularly in hot arid climates, at the cost of heavy irrigation, which is often a challenge in such climates.

However, similarly large energy savings can be achieved through other means as well. For example, Figure 8 shows the results from modeling the same single-story building as in Figure 7, but with added roof insulation of 3 m^2·K/W, or 8.6 cm of polystyrene foam, above the roof slab (ASHRAE 2005).

In addition to drastically reducing cooling and heating loads, insulation helps to even the energy performance of the three types of roofs. In climates dominated by heating energy, such as Minneapolis and Boston, the difference in energy consumption associated with each type of roof is much smaller, roughly 6% in Minneapolis. However, in climates dominated by cooling loads, such as Phoenix and Lisbon, both green and cool roofs can save up to 25% in total energy consumption. It should also be noted that in every climate the green and cool roofs now perform nearly identically, whereas the green roof outperforms the cool roof in every city in Figure 7. Both types of roof now perform similarly because the added insulation greatly limits heat transfer in both cases. With no added roof insulation, as in Figure 7, the dominating factor behind the green roof's high performance is the insulative effect of the soil. When 3 m^2·K/W of insulation is added, however, the insulative effect of the added insulation dominates that of the soil, thus heat transfer is mostly limited by the added insulation. Heat transfer through the cool roof is also limited by the added insulation, so both roofs perform similarly.

Effect of Insulation

To further investigate the effect of the amount of insulation on the energy-saving potential of cool and green roofs, the annual energy consumption of the building from Figure 7 is now plotted as a function of roof insulation R-value in Figure 9.

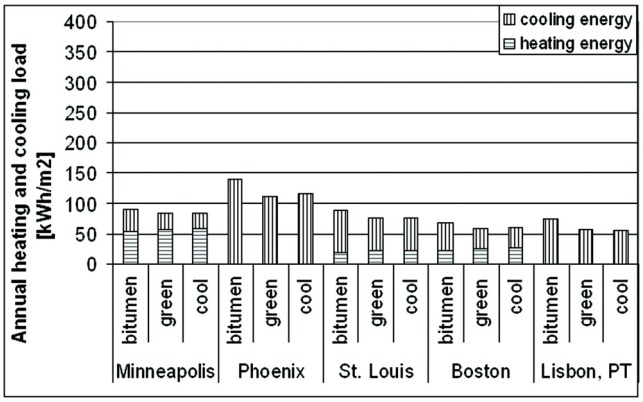

Figure 8 *Average annual primary energy required for heating and cooling for the same single-story building in Figure 7 with 3 m^2·K/W of roof insulation above the roof slab.*

As one might expect, the total energy use generally decreases as more roof insulation is added. What is perhaps less intuitive is the potential energy savings from adding insulation as compared to changing roof types. For example, consider a nonresidential building in Boston with a traditional modified-bitumen roof and 2.7 m^2·K/W insulation above the roof deck, which is slightly above the standard set by ASHRAE/IESNA Standard 90.1 for Boston's climate (ASHRAE 2004). Although installing a green roof or a cool roof would save 12% and 11% annually on heating and cooling energy, respectively, if the modified-bitumen roof is kept and the insulation is increased to 5.4 m^2·K/W, a 13% savings is realized. All three options yield similar energy savings, but at very different costs.

Lisbon presents an interesting case where there is a predicted optimum amount of roof insulation, approximately

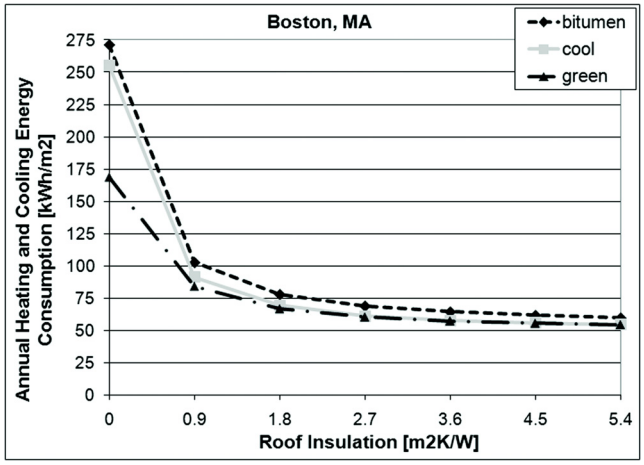

(a)

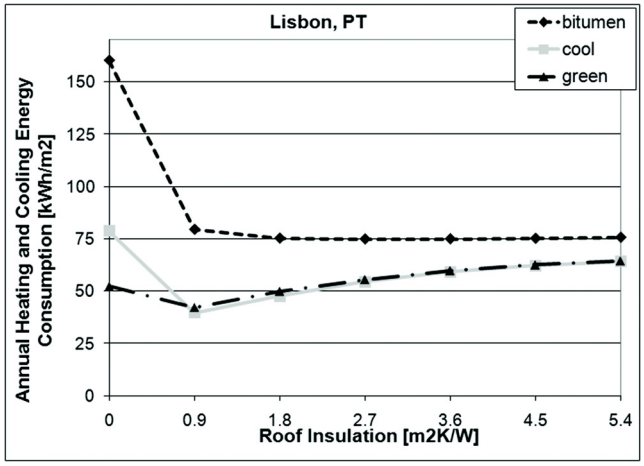

(b)

Figure 9 *Average annual primary energy required for heating and cooling for the same single-story building in Figure 7 plotted as a function of roof insulation above the roof slab.*

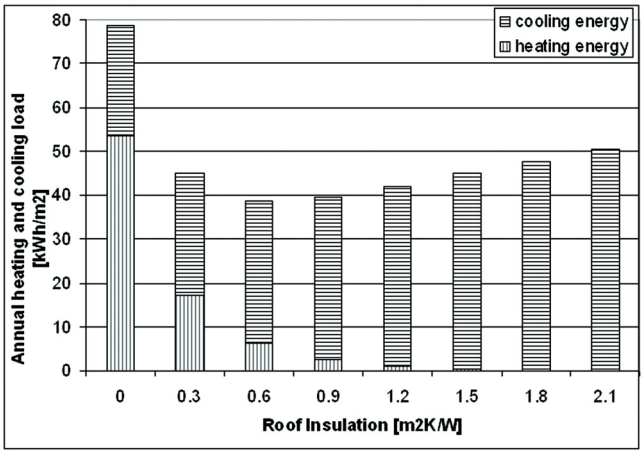

Figure 10 *Breakdown of heating and cooling energy of building in Lisbon with a cool roof shown in Figure 9b.*

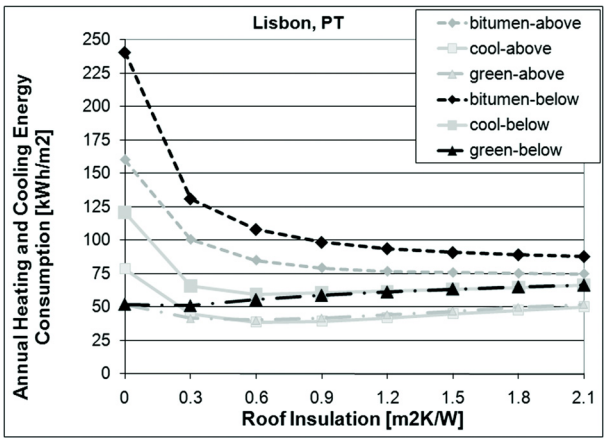

Figure 11 *Average annual primary energy required for heating and cooling for the same single-story building in Figure 7 plotted as a function of roof insulation above and below the roof slab.*

0.6 m^2·K/W, which is below the 2 m^2·K/W required by the Portuguese government (MPW 2006). This optimum low level of insulation arises as a result of decreasing heating energy but increasing cooling energy with insulation as shown in Figure 10.

As more insulation is added, the internal and solar gains are high enough to eliminate a heating load. Simultaneously, however, more insulation hinders the passive cooling from the cool roof, thus increasing cooling energy.

Insulation Location

The energy consumption of the building is affected by not only the amount of roof insulation but also the location of the insulation. Assuming a concrete roof slab is used, when the insulation is above the slab (top case) the thermal mass is exposed to the indoor air temperature, helping to moderate it and lead to lower energy demands, as shown in Figure 11.

Number of Floors

The number of floors of a building with a green or cool roof also impacts the net energy savings of the roof. The roof module to the MIT Design Advisor (MIT 2010) allows closer investigation into this impact. Figure 12 shows that the impact on area-weighted average energy consumption is essentially unaffected by changing roof types for buildings above six stories in Lisbon with roof insulation.

Further Comparisons

Countless similar simulations can now be made through the MIT Design Advisor (MIT 2010) that will shed light on the energy-saving impact of cool and green roofs. For example, a one-story building in Boston with a modified-bitumen roof and 2.7 m^2·K/W roof insulation can save 12% in cooling and heating energy by installing a green roof. If 2 in. of roof insulation

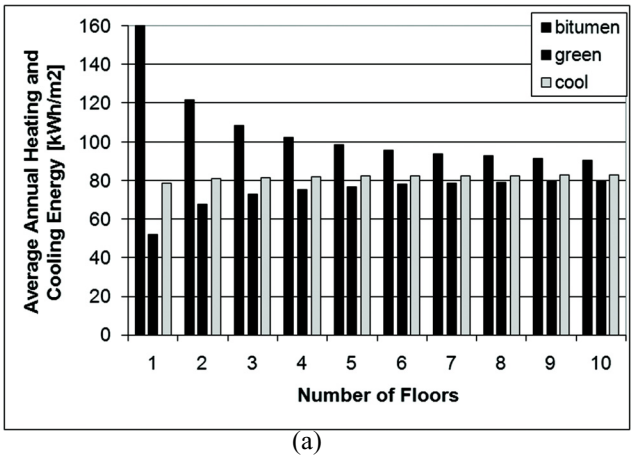

(a)

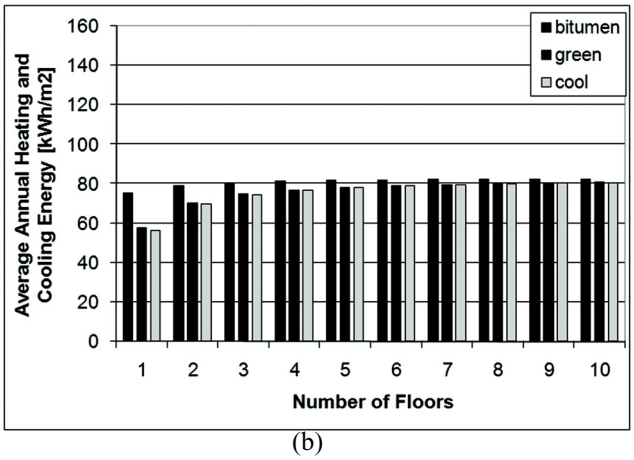

(b)

Figure 12 *Average annual primary energy required for heating and cooling a multi-story equivalent to the building in Figure 7 with a) no roof insulation and b) 3 m^2·K/W roof insulation as a function of number of floors in Lisbon.*

is added to the modified-bitumen roof, a savings of 13% are realized, often at a lower cost. However, in Lisbon, the same additional amount of roof insulation to the same building results in –0.01% savings, while the installation of a green roof with 2.7 m^2·K/W roof insulation results in a 26% reduction in energy use. These findings illustrate how the MIT Design Advisor helps to identify the most energy-efficient roof system for a given building and climate.

CONCLUSION

The need for a roofing tool that not only is simple and intuitive enough for nontechnical users but also is accurate enough to produce meaningful results is met by the roof module added to MIT's Design Advisor (MIT 2010). The first-principles-based cool and green roof models are shown to accurately predict $T_{surface}$, which in turn is used to estimate the energy flux through the roof.

The development of this tool allows quick analysis of alternative roof technologies in the early design stage. Comparisons between roof types and constructions can be made in locations throughout the world in minutes. Findings from the sample comparisons presented here are the following.

- Buildings with no roof insulation generally realize much higher energy savings by adding as little as 1 m^2·K/W roof insulation instead of installing a different kind of roof.
- Even for a heavily insulated roof, a 5%–10% savings can be realized if the proper roof is chosen.
- With roof insulation, cool roofs generally perform best in sunny and hot climates, while green roofs generally perform best in moderate to cold climates.
- Without roof insulation, green roofs are predicted to perform best, provided they are actively growing, because of the insulative properties of the growing media and potential passive cooling.
- Regardless of roof insulation, cool roofs nearly always decrease the cooling load but simultaneously increase the heating load.
- In certain climates, more roof insulation is not always better, especially if a green or cool roof is used.

Although not investigated in this study, numerous other factors must be considered when evaluating roofing decisions—potential energy savings clearly are not the sole driver of their use.

ACKNOWLEDGMENTS

This work was funded by the MIT Portugal Program, to whom the authors extend great appreciation. Similar gratitude is extended to Hideki Takebayashi of Kobe University and Jeff Sonne of the Florida Solar Energy Center for their collaboration with this work.

NOMENCLATURE

ET_0	=	evapotranspiration, mm/h
G	=	soil conductive heat flux density, MJ/m^2·h
$\bar{h}$	=	average heat transfer coefficient for roof surface, W/m^2·K
h_{rad}	=	radiation heat transfer coefficient, W/m^2·K
h_{room}	=	effective heat transfer coefficient between ceiling and room beneath roof, W/m^2·K
H_{veg}	=	convective heat transfer away from vegetation, W/m^2
H_{roof}	=	convective heat transfer from roof to environment, W/m^2
I_s	=	incident shortwave radiation, W/m^2
k_{ext}	=	extinction coefficient for vegetation
L_{veg}	=	latent heat transfer from vegetation, W/m^2
LAI	=	leaf area index
$p_{sat(T_{hr})}$	=	saturation vapor pressure at T_{hr}, kPa
P_{act}	=	average hourly actual vapor pressure, kPa
$q_{ir,roof}$	=	longwave radiation between roof surface and sky, W/m^2
R_n	=	net radiation at the grass surface, MJ/m^2·h
T_{amb}	=	ambient outdoor temperature, K
T_{hr}	=	mean hourly air temperature, K
T_m	=	average temperature of roof surface and sky, K
T_{room}	=	temperature of room beneath roof, K
T_{sky}	=	temperature of sky, K
$T_{surface}$	=	temperature of roof surface, K
T_{veg}	=	temperature of vegetation, K
u_2	=	average hourly wind speed 2 m above the vegetation, m/s

Greek Symbols

α	=	leaf absorptivity
γ	=	psychrometric constant, kPa/°C
Δ	=	saturation slope vapor pressure curve at T_{hr}, kPa/°C
ε	=	emissivity
ρ	=	roof surface reflectivity
σ	=	Stefan-Boltzman coefficient, W/m^2·K^4
τ	=	transmittance through vegetation

Subscripts

l	=	longwave
s	=	shortwave
veg	=	vegetation

REFERENCES

Alexandri, E., and P. Jones. 2007. Developing a one-dimensional heat and mass transfer algorithm for describing

the effect of green roofs on the built environment: Comparison with experimental results. *Building and Environment* 42(8):2835–49. doi:10.1016/j.buildenv.2006.07.004.

Allen, R., L. Pereira, D. Raes, and M. Smith. 1998. Crop evapotranspiration—Guidelines for computing crop water requirements. Tech. Rep. FAO Irrigation and drainage paper 56, Rome: Food and Agriculture Organization of the United Nations.

Allen, R.G. 2005. W.R.I.U. Environmental, The ASCE Standardized Reference Evapotranspiration Equation. Technical Report, American Society of Civil Engineers, Reston, VA.

ASHRAE. 2005. *ASHRAE Handbook—Fundamentals.* Atlanta: American Society of Heating, Refrigerating and Air-Conditioning Engineers, Inc.

ASHRAE. 2004. *ANSI/ASHRAE/IESNA Standard 90.1-2004, Energy Standard for Buildings Except Low-Rise Residential Buildings*. Atlanta: American Society of Heating, Refrigerating and Air-Conditioning Engineers, Inc.

Cummings, J., C. Withers, J. Sonne, D. Parker, and R. Vieira. 2007. UCF recommissioning, green roofing technology, and building science training. Final report, Tech. Rep. FSEC-CR-1718-07 and FSEC# 20127036, Florida Solar Energy Center, Florida (May).

Droogers, P., and R.G. Allen. 2002. Estimating reference evapotranspiration under inaccurate data conditions. *Irrigation and Drainage Systems* 16(1):33–45.

FSEC. 2008. Experiment database management system. www.logger.fsec.ucf.edu/cgi-bin/wg40.exe?user=baihppsp. Cocoa, FL: Florida Solar Energy Center.

GRHC. 2009. Greensave Calculator. www.green roofs.org/index.php/greensavecalc. Toronto, ON, Canada: Green Roofs for Healthy Cities.

JJH. 2003. DOE2.1-E. James J. Hirsch & Associates (JJH) in collaboration with Lawrence Berkeley National Laboratory (LBNL).

Jones, H.G. 1992. *Plants and Microclimate*. Cambridge, UK: Cambridge University Press.

Kite, G.W., and P. Droogers. 2000. Comparing evapotranspiration estimates from 27 satellites, hydrological models and field data. *Journal of Hydrology* 229(1-2):3–18.

Kumar, R., and S. Kaushik. 2005. Performance evaluation of green roof and shading for thermal protection of buildings. *Building and Environment* 40(11):1505–11.

LaFrance, M., W. Miller, J. Huang, and J. New. 2010. Calculating energy savings of cool roofs. Presentation for Building Technologies Program of U.S. Department of Energy, April 22.

Lazzarin, R.M., F. Castellotti, and F. Busato. 2005. Experimental measurements and numerical modelling of a green roof. *Energy and Buildings* 37(12):1260–67. doi:10.1016/j.enbuild.2005.02.001.

LBNL. 2010. EnergyPlus Engineering Reference. EnergyPlus Manual Documentation Version 5.0, April. The Board of Trustees of the University of Illinois and the Regents of the University of California through the Ernest Orlando Lawrence Berkely National Laboratory.

Lienhard IV, J., and J. Lienhard V. 2006. *A Heat Transfer Textbook*, 3d ed. Cambridge, MA: Phlogiston Press.

Martin, M., and P. Berdahl. 1984. Characteristics of infrared sky radiation in the United States. *Solar Energy* 33:321–36.

Mills, A. 1991. *Heat Transfer*. Boca Raton, FL: CRC Press.

MPW. 2006. RCCTE—Regulation for the Thermal Performance of Buildings, Law 80/2006 of the Portuguese Republic Diary. Lisbon, Portugal: Portuguese Government, Ministry of Public Works, Transport and Communications.

MIT. 2010. MIT Design Advisor. http://designadvisor.mit.edu. Cambridge, MA: Massachusetts Institute of Technology.

NWS. 2009. National Weather Service Web site, Arizona precipitation page. www.wrh.noaa.gov/psr/DroughtPage.php?wfo=psr&data=ALLDATA.

Niachou, A., K. Papakonstantinou, M. Santamouris, A. Tsangrassoulis, and G. Mihalakakou. 2001. Analysis of the green roof thermal properties and investigation of its energy performance. *Energy and Buildings* 33(7):719–29.

Petrie, T.W., and K.E. Wilkes. 1998. Effect of radiant barriers and attic ventilation on residential attics and attic duct systems: New tools for measuring and modeling. *ASHRAE Transactions* 104:1175–92.

Ray, S. 2010. Energy saving potential of various roof technologies. Mechanical Engineering SM thesis, Massachusetts Institute of Technology, Cambridge, MA.

Russell, G., B. Marshall, and P.G. Jarvis. 1990. *Plant Canopies: Their Growth, Form and Function*. Cambridge, MA: Cambridge University Press.

Sailor, D. 2008. A green roof model for building energy simulation programs. *Energy and Buildings* 40(8):1466–78.

Santamouris, M., C. Pavlou, P. Doukas, G. Mihalakakou, A. Synnefa, A. Hatzibiros and P. Patargias. 2007. Investigating and analysing the energy and environmental performance of an experimental green roof system installed in a nursery school building in Athens, Greece. *Energy* 32(9):1781–88.

Smith, J. 2004. Building energy calculator: A design tool for energy analysis of residential buildings in developing countries. Mechanical Engineering SM thesis, Massachusetts Institute of Technology, Cambridge, MA.

Sonne, J. 2006. Evaluating green roof energy performance. *ASHRAE Journal* 48(2):59–61.

Sonne, J. 2008. Personal communication with the author (email). "Re: FSEC web site message from Steve Ray." 19 Dec.

Strang, G. 2007. *Computational Science and Engineering.* Wellesley, MA: Wellesley-Cambridge Press.

Suleiman, A.A., and G. Hoogenboom. 2007. Comparison of Priestley-Taylor and FAO-56 Penman-Monteith for daily reference evapotranspiration estimation in Georgia. *Journal of Irrigation and Drainage Engineering* 133(2):175–82.

Takakura, T. 1993. *Climate Under Cover: Digital Dynamic Simulation in Plant Bio-Engineering*. Berlin: Springer.

Takakura, T., S. Kitade, and E. Goto. 2000. Cooling effect of greenery cover over a building. *Energy and Buildings* 31(1):1–6.

Takebayashi, H., and M. Moriyama. 2006. Surface heat budget for green roof and high reflection roof for urban heat island mitigation. 6th International Conference on Urban Climate, Goteborg, Sweden, June.

Takebayashi, H., and M. Moriyama. 2007. Surface heat budget on green roof and high reflection roof for mitigation of urban heat island. *Building and Environment* 42(8):2971–79.

Teh, C. 2006. *Introduction to Mathematical Modeling of Crop Growth*. Boca Raton, FL: Brown Walker Press.

Theodosiou, T.G. 2003. Summer period analysis of the performance of a planted roof as a passive cooling technique. *Energy and Buildings* 35(9):909–17.

Urban, B. 2007. The MIT Design Advisor: Simple and rapid energy simulation of early stage building designs. Mechanical Engineering SM thesis, Massachusetts Institute of Technology, Cambridge, MA.

WU. 2008. Weather Underground Web site, www.wunderground.com.

Wong, N.H., D.K.W. Cheong, H. Yan, J. Soh, C.L. Ong, and A. Sia. 2003. The effects of rooftop garden on energy consumption of a commercial building in Singapore. *Energy and Buildings* 35(4):353–64.

Zhang, J.Q., X.P. Fang, H.X. Zhang, W. Yang, and C.C. Zhu. 1997. A heat balance model for partially vegetated surfaces. *Infrared Physics & Technology* 38(5):287–94.

Zhu, W., and D. Schultz. 2009. National Severe Storms Laboratory (NSSL) Historical Weather Data Archive. http://data.nssl.noaa.gov/credits.html.